Development of Hardness Distribution, Thermal, and Tensile Analysis of Resistance Spot Welding

Shraddha Bajpai, M. Tech Scholar, Department of Mechanical Engineering, Kanpur Institute of Technology, Kanpur, India.
Dr. Vivek Srivastava, Professor, Department of Mechanical Engineering, Kanpur Institute of Technology, Kanpur, India

Abstract— **Process planning is more important than ever in production engineering because it enables process optimization, which saves costs, has a smaller environmental impact, and uses time more efficiently. Widespread usage of resistance spot welding (RSW) as a large-scale joining technology shows process optimization is possible.**
This thesis seeks to improve RSW process planning in industrial applications. The objective is expressed by two study topics: process variance and numerical techniques for RSW. Research questions are centred on weld size in RSW process planning.
Weld size changes due to process parameters and unintentional fluctuations in welding circumstances, as with any large-scale production process. Physical and numerical analyses have been done to comprehend such oscillations.
Both laboratory and industrial welding were used to explore unintended variances that contribute to varied weld thicknesses in seemingly identical conditions. The study revealed weld sizes and standard deviations in each environment. Weld sizes match the Normal and Weibull distributions, and standard deviations in industrial production and controlled laboratories are 0.3 mm and 0.9 mm, respectively.

Index Terms— Resistance Spot Welding, Heat, Friction, Temperature, Tensile strength, Tool pin profile, welding speed, etc

I. INTRODUCTION

The automotive business is regularly troubled to boost fuel potency by using light-weight materials like Al and Mg alloys, since reducing vehicle weight will greatly lower fuel consumption. With the multiplied use of Al and Mg, there's a pressing want for a technology to supply dissimilar Al/Mg joints, and ideally by RSW since this technology is presently predominant within the business. To-date the matter of connection Al and Mg remains open. The most important problem in attachment of Al to Mg is formation of exhausting and brittle intermetallic compounds that have a prejudicial impact on the joints strength. Currently, the foremost promising approach to resolve this drawback is using interlayer which may improve microstructure and mechanical performance of Al/Mg welds. Terribly restricted info on RSW of Al to Mg is out there within the literature whereas there's no Associate in nursing info on RSW of Al to Mg with a bed. Therefore, it's essential to explore effects of various interlayers on dissimilar Al/Mg resistance spot welds to fill the gap between RSW and alternative connection techniques in quantity of data offered on the topic and promote farther implementation of sunshine alloys within the automotive business.
RSW may be a attachment technique {in that during which within which} the faying sheets of metal are joined during a spot by the warmth made because of resistance to the electrical current which passes through coupons squeezed from prime and bottom by electrodes. the essential RSW method involves many consecutive steps: clamping electrodes to tightly press attachment coupons together; applying attachment force that is considerably beyond initial compressing force; applying attachment current that results in melting of coupons in weld zone; holding coupons with bound force whereas fusion zone solidifies; unclamping of the electrodes. A schematic sketch of RSW of 2 sheets is shown on figure 1.

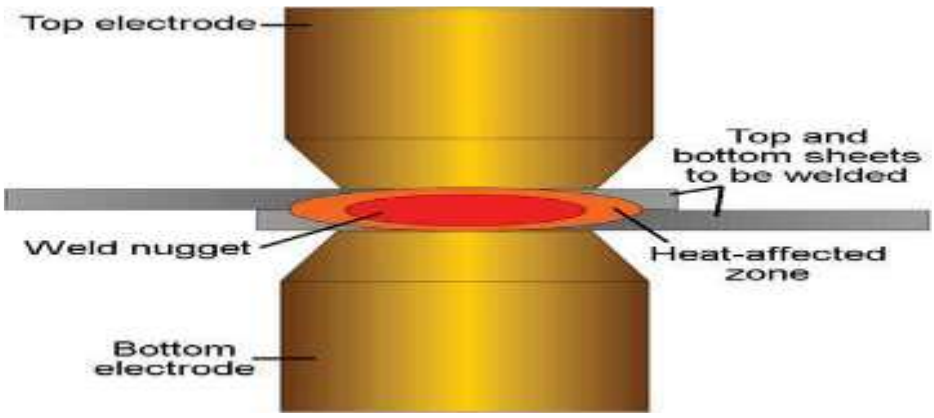

Figure 1: Schematic sketch of RSW of 2 sheets [1] (reprinted with permission of ASM International)

RSW is that the primary connection technique for several flat solid applications, using this attachment technique is efficient, quick and may be simply machine-driven. Sheets with thicknesses up to three.2 millimeter are joined by this method, that suits most applications since the bulk of business assemblies involve sheets with thicknesses but three millimeter. RSW conjointly permits one to supply spot joints of multiple sheets stacks, wherever the number of sheets within the stack is sometimes less or adequate 5. The most important limitation of RSW is that solely joints in overlap configuration are made by this method. However, flat solid connection in overlap configuration is needed for several applications in sort of industries [2, 3]. As an example 5,000 resistance spot welds performed in producing Associate in Nursing automobile [4].

Weld nugget formation and sheet thickness

In RSW, two workpieces are stacked together between two electrodes by applying force. During the welding process, parameters like weld current, electrode force and weld time are set to a specific value for welding various thicknesses and materials. A physical phenomenon in resistance spot welding as the current is passing through the sheets, the resistances of the circuit cause generation of heat energy. A Joule's law given in equation (1) is used to estimate heat energy supplied during welding operation for melting the material.

$$Q = \eta \int_0^T I^2 R dt \quad (1)$$

Where, Q is the energy supplied, I, R and η are the welding current, resistance and weld efficiency respectively. The heat generation raises the materials' temperature above the melting point mainly due to surface resistances between the sheets. After the metal sheets have molten the current is stopped and no further heat is generated. The figure 2 shows the contribution of process parameters on nugget formation. Nugget is a function of electrode force, welding current, weld time, size and contour of the electrode tip, sheet thickness and work piece' resistance. The current flow across the electrodes is a function of the force applied on the workpieces to obtain sufficient heat to raise a confined volume of metal to a molten state in sequence. The acceptable weld joints were produced by selecting an appropriate combination of process parameters.

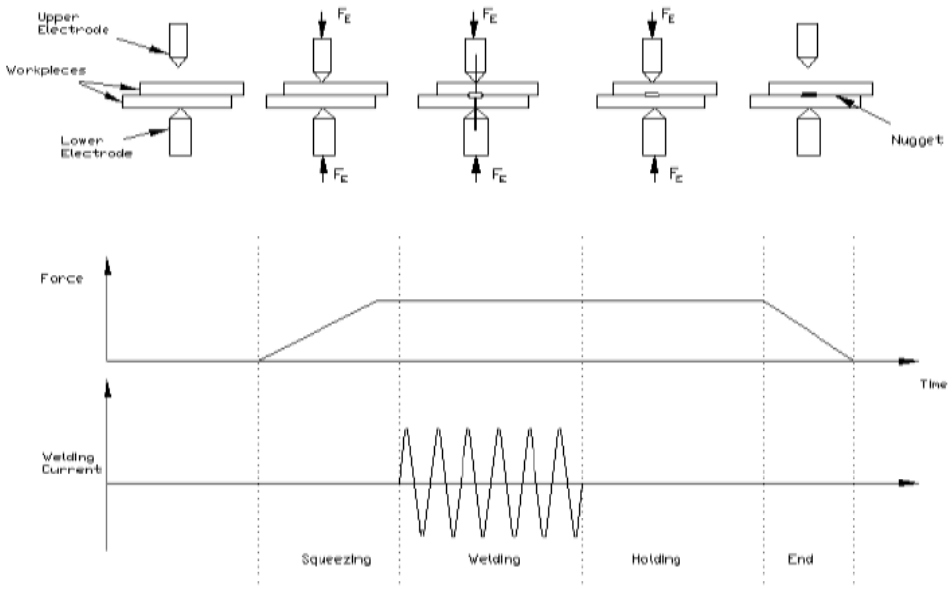

Figure 2: Spot Welding Stage

The metal can cool, consequently leading to the formation of the nugget on cooling under pressure in a controlled manner to avoid the very high temperature leading to the expelling of the molten metal from the weld. The excessive heating of the electrode faces can be prevented by supplying the current for a short duration. The region which melts and solidifies is called a nugget. The standard relationship between weld force and other parameters is represented in equation (2), (3) and (4).

$$F_w = 250 t_w \quad (2)$$

$$F_w = \frac{P_w \rho L}{R} \quad (3)$$

$$F_w = \frac{P_w \rho L I^2}{P_p} \quad (4)$$

Where, F_w, t_w, p_w, ρ, L, R, I, and p_p are the weld force, weld time, weld power, density, weld length resistivity of the material, current and peak power respectively.

The welding input parameters directly influence a weld joint's quality during the welding process; therefore, welding can be considered a multi-input multi-output process. In many manufacturing industries, figure 3 shows various defects, like Nugget diameter, Deep spot, Tensile Shear Strength, Spatter, Burr, Miss Spots, Weak spot, Spot Burn, were observed from many manufacturing industries during spot welding process due to improper setting of input parameters. The electrode force plays a significant role in maintaining the nugget diameter of the weld. As the electrode force increases, the heat energy input decrease, which means the higher the electrode force, the higher the welding current. As the pressure is increased, the contact resistance and the heat generated at the interface decreases. The contact resistance increases with increasing weld force, the spots are depressed and the actual metalto-metal contact area also increases. If the electrode force is gradually increased, increasing the contact surface's size during welding can be prevented, results in the same conditions. The average value is chosen to change the electrode force at the same rate as the electrodes are "mushroomed."

Figure 3: Defects in resistance spot welds

The metals to be joined in spot-welding are often different, or the thicknesses of the sheet of the sheets to be joined are different and it may be vice versa. Thus, it is necessary to keep the weld nugget symmetrical about the interface between the sheets, but there is no problem if the sheets are of the same thickness and of the same metal. Hence, we realize that the nugget will extend the same depth into both sheets intuitively. However, it is not hard to formulate the general conditions required for the symmetry of the nugget.

Weld nugget symmetry requires the heat generated in both plates to be the same, and the heat transfer out of the plates to be the same; the first requirement means that the two sheets' electrical conductance must be equal since the heat is generated by electrical resistance. The equality of heat loss means that the thermal conductance of both plates must be the same.

The electrical conductance and the thermal conductance are given by

$$G = \frac{g}{l} \times AK = \frac{k}{l} \times A \quad (5)$$

Where, l is sheet thickness and A is the electrodes connect area, G and g are electrical conductance and electrical conductivity, respectively. K and k are the corresponding thermal conductance and thermal conductivity, respectively. If we are looking with the same metal but with sheets of different thickness, equation (5) gives the requirements for electrode area in terms of relative sheet thickness.

$$K_1 = \left(\frac{k_1}{l_1}\right) A_1 \ , \ K_2 = \left(\frac{k_2}{l_2}\right) A_2 \quad (6)$$

Since we want, $K_1 = K_2$. So $\left(\frac{A_1}{l_1}\right) = \left(\frac{A_2}{l_2}\right)$ or we have $\left(\frac{l_1}{l_2}\right) = \left(\frac{A_1}{A_2}\right)$.

In other words, the electrode areas against each plate must be proportional to the thickness of the sheet. A large electrode will then be placed against the thicker sheet. In effect, the largest electrode provides a large heat sink so that the weld nugget will be centralized at the interface. Equation (1-6) has neglected the heat leak into the plates through the ends of the nugget. However, this heat leak is approximately proportional to the heat leak to the electrodes. The conditions for spot welds between the sheets of like thickness but unlike metals are still governed by equation (5). In this case l_1=l_2.

$$\left(\frac{g_1}{g_2}\right) = \left(\frac{A_1}{A_2}\right) \quad (7)$$

When spot welding thickness sheets are used, the electrode areas should be inversely proportional to the conductivity. For most pairs of metals, the electrical conductivity of each has the same ratio as the thermal conductivity of other. Therefore, the ratio g_1/g_2 may be either the ratio of the thermal or the electrical conductivity. The dissimilar metals of dissimilar thickness sheet, $g_1 \neq g_2$ or, $l_1 \neq l_2$, therefore the equation (7) can be modified and written as,

$$\left[\frac{g_1}{l_1}\right] A_1 = \left[\frac{g_2}{l_2}\right] A_2 \; or \left[\frac{g_1/l_1}{g_2/l_2}\right] = \frac{A_2}{A_1} \quad (8)$$

The g/l ratio of each metal sheet determines the appropriate electrode area. A current is the most critical parameter significantly affecting the heat generation during spot welding. It is controlled by setting the transformer tap switch, which determines the amount of weld current made available and the percentage of current control determines the percentage of available current to be used for making the weld. A low percentage of current is not recommended as it impairs the quality of the weld. The current value for welding operation is finalized by increasing the current supply until weld spatter appears on the weld. The current has a significant influence on the amount of heat generated and tensile shear strength. Due to rapid increase in the current results in excessive melting of base metal, material expulsion, weld cracking and reduced mechanical strength. The excessive current will overheat the base metal and result in deep indentations in the parts. Besides, if the welding current becomes too high, spatter will occur between electrodes and sheets, causing the electrodes to get stuck the sheet.

Mg and Al Alloys

The automotive business is regularly troubled to boost fuel potency by using light-weight materials like Al and Mg alloys, since reducing vehicle weight will greatly lower fuel consumption. it had been reported that a hundred kilo of reduced vehicle weight saves concerning 0.3 L of fuel per a hundred metric linear unit [5]. though some Al-based frame structures are already made, utilization of those alloys has typically been progressive and resulted in styles that use multiple materials, which regularly got to be joined in dissimilar combos.

Connection of Al to Mg

Since, Al and Mg alloys will each be doubtless employed in an equivalent structure the matter of connection these 2 materials should be self-addressed. Various studies relating to dissimilar connection of Al to Mg by totally different techniques is found within the literature. The common drawback with all fusion-based dissimilar metal connection techniques of Al to Mg is that the formation of exhausting and brittle intermetallic compounds [6, 7]. Solid state processes that involve relatively low temperatures like diffusion bonding [8, 9], but friction stir attachment (FSW) [10-12] and a few others can do comparatively high strength, but even during this case formation of brittle Al-Mg intermetallic compounds cannot be fully avoided. Additionally solid state attachment techniques like friction stir attachment have vital limitations and weren't wide adopted by automotive and alternative production industries.

To mitigate the formation of undesirable intermetallics, some work has been done to explore the impact of various interlayer on the properties of Al/Mg joints. a spread of interlayer like atomic number 30 [13], Ce [14], Ag [15], Sn [16], Ti [17], Cu [18], Ni [12, 19] et al. were incorporated with totally different solid- and non-solid state attachment processes. In general, using interlayer reduced fraction of Al-Mg intermetallics and improved mechanical properties of the joints.

RSW of Al to Mg is especially attention-grabbing since it's the predominant connection technique within the automotive business. Nonetheless, only 1 elaborate study on RSW of Al to Mg is out there within the literature [19,20]. The strength of the welds achieved during this study was negatively influenced by formation of brittle intermetallic compounds. Additionally this study thought-about commercially pure Al that inevitably would end in low strength joints because of fracture propagation through the soft base metal additionally. Therefore, an appropriate technology for achieving high strength Al/Mg welds by RSW has nonetheless to be developed.

Considering info offered within the literature, using Associate in nursing bed throughout attachment of Al to Mg may well be a possible approach to eliminate intermetallics and improve mechanical properties of the joints throughout RSW.

Interlayer Used

RSW of Al to Mg with six totally different interlayer was performed within the current study. As are often seen from Table 1 welds created with 3 totally different interlayer met necessities of AWS D17.2 standard. Ni-based interlayer and Zn-coated steel were chosen to be analyzed in details within the current study. Transient info on RSW with different interlayer summarized within the appendices. Despite the actual fact that welds created with Sn-coated steel bed additionally met necessities of the quality, it absolutely was complete that Zn-coated steel is additional necessary to analyze, since it's rather more common material and far lower price than Au-coated Ni.

Table 1: List of materials used as interlayer for RSW of Al/Mg within the current study

Interlayer	Lap shear strength met requirement of AWS D17.2 standard [20]
Au-coated Ni	Yes
Ni foil	No
Sn-coated steel	Yes
Zn-coated steel	Yes
Zn foil	No
Cu foil	No

II. Literature Review

Many researchers have contributed to improve the weld quality and strength by conducting experiments on similar and dissimilar metals of different thickness by varying weld process parameters. Some of the prominent publications, and their contributions to the fabrication of dissimilar metal structures the spot welding are listed below,

Resistance spot welding for Similar Material

In the automotive industries, weight reduction is strongly demanded energy and natural resource savings. Due to low density and significant mechanical properties, a lightweight metal such as aluminum alloys and magnesium alloys has been adopted. They are expected to be extensively used to replace steel, which is partially the automobile's primary construction material. On the other hand, resistance spot welding (RSW) is a widely used and essential welding process in automotive manufacturing because it is economical, fast and robust to part tolerance variations. The RSW of steel, which has been extensively investigated, investigates the RSW of these lightweight metal sheets as indispensable.

In recent literature, D. Q. Sun et al., have studied the microstructures and mechanical properties of joint [21]. Y. R. Wang et al., [22] have studied the effect of welding time on the microstructure and tensile shear load of joints. B. Lang et al., [23] have investigated the optimization design of RSW parameters of magnesium alloy. Concerning the RSW of aluminum alloys, numerous researches have been reported so far. For example, Y. Imamura and S. Sasabe have investigated Al-Mg alloy's continuous spot weld ability [24]. D. K. Aidun and R. W. Bennett have studied the effects of welding parameters on the strength of aluminum alloy 6061-T6 joint [25]. P. H. Thornton, A. R. Krause and R. G. Davies have investigated the relationship between fatigue strength and nugget diameter of aluminum alloy joint [26]. L. Xu and J. A. Khan have related the nugget growth process during the RSW of aluminum alloy [27].

A. Gean, S. A. Westgate, J. C. Kucza and J. C. Ehrstromhave stated the influence of porosity on the static and fatigue strength of aluminum alloy joints. These experiments provided useful information to understand the performance of the magnesium alloys joint and aluminum alloys joint and revealed that enormously high welding current. 2.5 to 3 times the current of welding steel is required in these alloys' RSW process due to their high electrical and thermal conductivity.

However, an enormously high welding current would cause two problems. Firstly, electrode tips wear: The electrode/sheet interfaces' resistance is partially due to an oxide coating on the base metal sheet's surface, mainly aluminum alloy. The oxide acts as an insulator at the electrode sheet interfaces and creates problems for the RSW process. When the current is applied, it seeks the path of least resistance, where the oxide has been broken up. This leads to uneven current distribution and excessive localized current density, resulting in uneven heating. Due to local melting at the interface and alloying results, surface discontinuities because accelerated electrode surface deterioration. A higher welding current would intensify the electrode tip erosion.

Secondly, an enormously high welding current would require installing a larger capacity RSW machine. Since available welding current for RSW of steel is between 6 kA and 12 kA. S. Aslanlar, A. Ogur, [28] and O. Martin P.D. Tiedra studied [29], the rating capacity of RSW machines equipped in assembly lines of a steel-structural automobile body is usually low. Using this welding equipment cannot attain the enormously high current welding. Methods commonly used in steel that extend the welding time to produce a weld are not effective for aluminum or magnesium because most weld development occurs during the first half of the weld cycle in these materials instead of the latter half for steel. Thus, a new weld system must be installed to deliver higher current levels than what is commonly employed for steel.

Naturally, this is unacceptable. Therefore, it would be practical to weld the lightweight metal such as aluminum alloy and magnesium alloys under the welding condition of low welding current using RSW machines with low rated capacity. Summary of the similar metals joint RSW with cover plates investigated the effects of welding parameters on the tensile shear strength of the joint and the shape characteristic of a nugget. To better understand the resistance spot weldability, these lightweight metals provide some foundational information for improving the lightweight metal joints' mechanical properties. Identified pore formation mechanism during resistance spot welding of these lightweight metal sheets to remedy this problem.

Resistance spot welding for Dissimilar Materials

A The need for joints between dissimilar materials often arises in the industries, especially automotive industries, because good joints between dissimilar materials enable multi-material design methodologies and low-cost fabrication processes. From this point of view, material supply, steels and lightweight materials such as aluminum alloys, magnesium alloys and titanium alloys are the most important construction materials. Therefore, the sound joining techniques among them are indispensable. However, these dissimilar materials joining have some difficulties in the welding process because of the massive difference in physical and thermal properties and brittle reaction products at the welding interface. They were divided into several types according to their characteristic. Author investigated the weld joint characteristics by joining of aluminum alloy, either with steel titanium/aluminum /magnesium alloy. Thus far, numerous researches concerning the joining of HA+LB type materials combination have been reported. However, most previous studies have focused on solid-state bonding to suppress interfacial reactions, such as friction welding, magnetic pressure welding, roll bonding, friction stir welding and diffusion bonding. On the other hand, RSW is a widely used and essential welding process in

automotive manufacturing; nevertheless, only a few studies have been reported on the RSW of HA+LB type materials combination to date. This is because conventional RSW is an authorized fusion welding process. The interfacial reaction cannot be suppressed if using conventional RSW to weld these types of dissimilar materials combinations. In several studies concerning the RSW of HA+LB type materials combination. The welded 1.0 mm Al-Mg alloy sheet 0.8 mm steel sheet Sun X. et al., [30]. Welded 1.4 mm SAEIO 08 mild steel sheet and 2 mm 5182-O aluminum alloy sheet. They introduced an aluminum-clad steel sheet between aluminum alloy and steel as the transition material to suppress the reaction between aluminum and steel. However, the welding process's utilization is still restricted by the aluminum-clad steel sheet's high cost and manufacturing difficulties. Therefore, a new method developed termed RSW with a cover plate for joining of HA+LB type materials combination. In the welding process, only the base material LB, which is covered by a plate with high resistance, is molten; consequently, solid-liquid joining is achieved.

This study joined steel/aluminum, titanium/aluminum, steel/magnesium and titanium/magnesium. It investigated the interfacial microstructure and analyzed the reaction layer's effect on the tensile shear load of joints. In this study, they welded steel/aluminum, titanium/aluminum, steel/magnesium and Titanium/magnesium using a newly developed technique of RSW with a cover plate. The interfacial microstructure and tensile shear strength of joints analyzed the reaction layer's effect on the tensile shear strength of joints. The joint performance was evaluated by the interfacial microstructure and tensile shear load of joints. The relationship between the reaction layer and tensile shear strength was also discussed. The results suggest that the RSW with a cover plate is feasible to weld these dissimilar materials combinations. These dissimilar materials joining are attained under the same welding conditions as joining of steels. Therefore, RSW with a cover plate would bridge the gap between the joining of steels and the joining of these dissimilar materials in the welding condition.

Material Choice

Welding specimens employed in this study were commercially obtainable sheets of Mg alloyAZ31B-H24 and Al alloy 5754-0. Dimensions of the Al and Mg alloy fastening coupons were a hundred x thirty five millimeter x two millimeter. Nominal composition and basic mechanical and physical properties of both alloys employed in the study square measure summarized in Table 2 and Table 3 severally. The surface of the Mg sheets was treated with answer of 2.5 g chromic chemical compound and a hundred milliliter water prior to fastening, and therefore the Al coupons were ultrasonically clean in grain alcohol for ten minutes and treated with answer of 1.2 mL HF, 67.5 milliliter HNO3 and a hundred milliliter water.

Table 2: Chemical composition of Al and Mg alloys employed in this study in wt.%

	Al	Mg	Si	Fe	Mn	Zn	Cr
Mg AZ31B	3	3 Bal.	0.1	-	0.2	-	-
Al 5754	Bal.	3	0.4	0.4	0.5	0.2	0.3

Table 3: Basic properties of Al and Mg alloys employed in this study

	Ultimate Tensile Strength, MPa	Electrical Resistivity, nΩ·m	Thermal Conductivity, W·m−1·K−1
Mg AZ31B-H24	285	92	96
Al 5754-0	215	49	147

Interlayer

Ni-based Interlayer

Pure Ni foil was used as associate bed during this study, in either associate uncoated condition or with associate electrolytic Au plating generally four to six to six thickness. Dimensions of the Ni-based interlayers were ten millimeter x ten millimeter x 0.2 mm. clean Ni interlayers were ultrasonically clean in acetone for ten minutes previous the fastening whereas Au-coated Ni was employed in as-received condition.

Zn-coated Steel bed

Another style of bed that was employed in this study is hot-dip galvanized HSLA steel. Composition of the steel is summarized in Table 4. Thickness of metal coating was approximately ten on either side. Zn-coated steel interlayers were larger than Ni-based interlayer, precise dimensions are: twenty millimeter x twenty millimeter x 0.7 mm. Before, the fastening Zn-coated steel was ultrasonically clean in ketone for five min.

Table 4: Chemical composition of the hot-dip Zn-coated steel used as associate bed(wt.%)

C	Mn	Si	Al	Cr	Ni	Cu	Nb
0.06	0.62	0.23	0.04	0.04	0.01	0.04	0.02

As evident in literature [31] and was delineate in this section, all hot-dip galvanized steels have nanoscale layer of Fe-Al intermetallic between metal coating and steel surface. Figure 4 shows Zn/steel interface of the bed employed in this study.

Increase of Al content between metal and steel proves that nanoscale layer of Fe-Al intermetallic, was also present within the steel employed in the {present this} study.

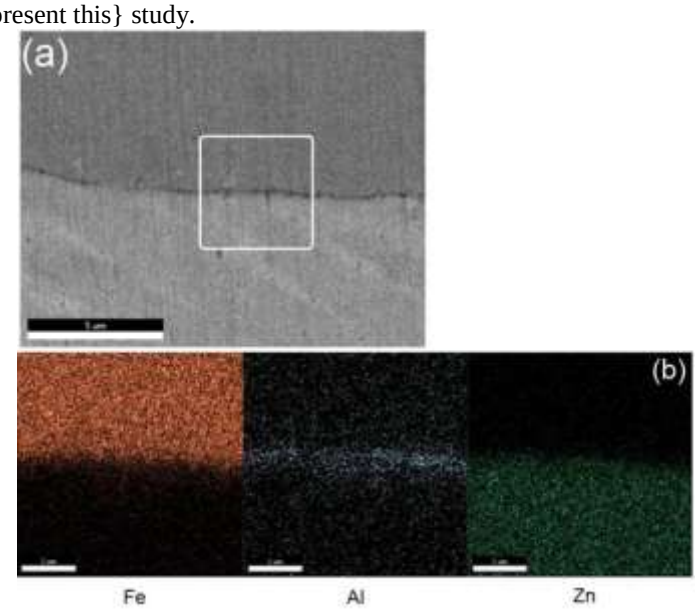

Figure 4: Interface between steel and metal coating in HSLA hot-dip galvanized steel. A SEM micrograph; b metal, Al and component metal} element distribution maps of space marked

Fastening Instrumentality

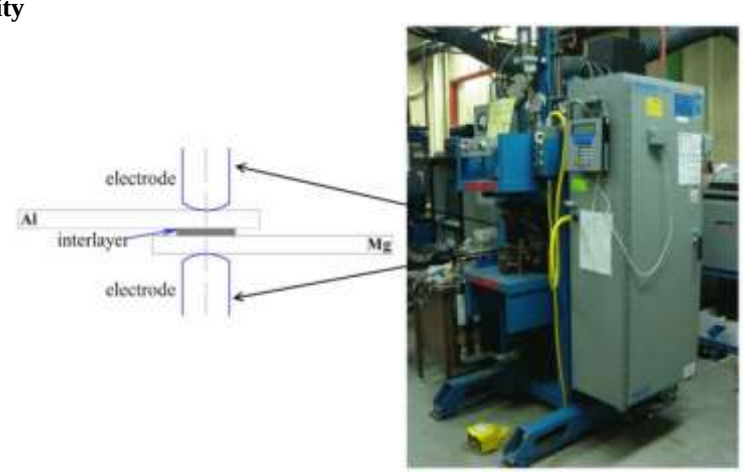

Figure 5: RSW machine and a schematic of the fastening coupons being joined

Welding parameters employed in the study square measure summarized in Table 5. Conductor caps sort FF25 were used and had a spherical radius of 50.8 millimeter and face diameter of sixteen millimeter, manufactured from Cu–Cr–Zr alloy. It ought to be noted that fastening current was the sole variable welding parameter during this study and it ranged from sixteen to twenty four Hindu deities for Ni-based interlayer and from 16 to thirty two Hindu deity for Zn-coated steel interlayer. Fastening currents over twenty four Hindu deity weren't tested for Ni-based interlayer, because of little size of the Au-coated Ni sheets obtainable for the experiments. Schematic of the standard fastening schedule employed in this study is shown on Figure 1.

Table 5: fastening parameters used for RSW of Al to Mg with interlayers

Squeeze Force, kN	Squeeze Time	Welding Force, kN	Welding Force Time	Welding Current, kA	Welding Time	Hold Time
2	30 cycles (0.5s)	4	30 cycles (0.5s)	16; 20; 24; 28; 32	5 cycles (1/12s)	30 cycles (0.5s)

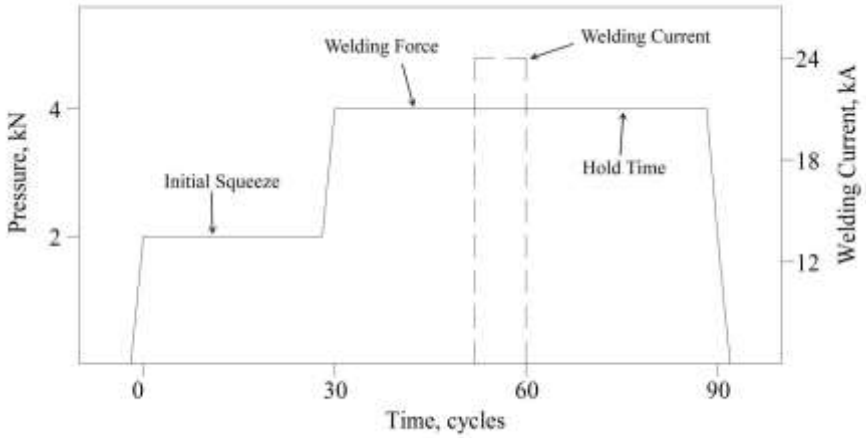

Figure 6: Full fastening schedule employed in the present study

Mechanical Testing

Three samples per condition were tested via tensile shear loading with fastening currents 16 and twenty Hindu deities whereas six samples tested with fastening currents of twenty four, twenty eight and thirty two Hindu deity. An Instron 4206 (Norwood, MA) tensile check machine was employed in this study, wherever specimens were strained to failure with a cross head speed of one mm/min. The pure mathematics of the fastening coupons for tensile shear check yet because the check set-up square measure shown on Figure 7. Alignment spacer sheets were accustomed grip the samples throughout overlap shear testing to reduce the bending or misalignment effects.

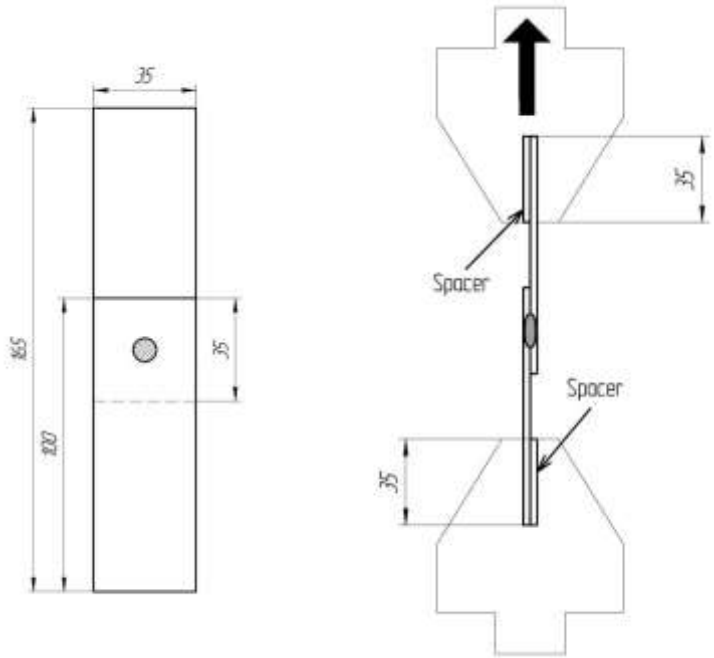

Figure 7: check coupon pure mathematics and tensile shear check set-up

Leco MHT series two hundred Vickers micro hardness tester was used for micro hardness evaluation. Check was performed on diagonal across the weld from high coupon to bottom coupon (Figure 7), like prescribed by AWS D8.9 standard. Every indent was created with a 100 g load and fifteen sec indentation time. Distance between every menstruation was adequate 0.254 millimeter (1/10") that was continuously larger than thrice the typical of any 2 adjacent indents.

Regression models of RSW

Regression models are a numerical model which uses statistical relations between a known set of input parameters (X) and output result (Y) to form a general model between the two general sets (x, y) with a set of constant coefficients (c). A regression model may be in the form shown in equation (9).

$$y = c_1x_1 + c_2x_2 + \ldots + c_nx_n \quad (9)$$

Regression models of the RSW process have to some degree been subject to research [21], [22], [23]. However, these models only treat only one material each and are thus not ready for a larger scale industrial implementation.

The regression model is generated through a least-square fitting, by the known set of input data and results, (X, Y) as shown in equation (10) [24].

$$c = (X^T X)^{-1} X^T Y \quad (10)$$

In in equation (10), the matrix X includes the known factors and the matrix Y includes the known results.
In RSW process planning, the most important measurement is weld nugget size and its sensitivity to process parameters. Thus, the regression model should describe the effects of changes in process parameters to weld nugget size [32]. The benefits of a regression model is the mathematically simplicity of the numerical model, while having high predictive capability if generated correctly.
The factors known to affect the weld nugget size are many and are often dependent of each other. The factors included in the regression model should satisfy several qualities; they should be physically and statistically significant while being easily accessible for process planning.

Finite element modeling for RSW simulations

Due to the complex multi-physical phenomena in the RSW process the FE simulations must be carefully formulated. More specifically, the coupled electricalthermal-mechanical coupling is of particular concern. In the following Chapter, the general modeling approaches and coupling, the governing equations of the model and the boundary conditions of the mesh are presented.
The first research work in RSW modeling [25] focused on one-dimensional models of the temperature distribution of the RSW process. Later the first axi-symmetrical model was developed [26]. Later axi-symmetrical models also measured the contact diameter between the sheets [27]. Research continued with a one dimensional model which took the temperature dependence of resistance into account [28]. Other axi-symmetrical models took the contact pressure dependence of contact resistance [29] or the steel hardness dependence of contact resistance [33] into account. A one-dimensional model was developed which measured weld size through temperature dependent contact resistance and material properties [34]. These earlier models were based on the Finite Difference Method, which limited their accuracy.

Electro-thermal-mechanical Coupling

In practice the coupled models are executed in small time-steps where, in each time step, the electro-thermal computations are made and used as input for the thermo-mechanical computations. A schematic illustration of the coupling can be seen in Figure 8.

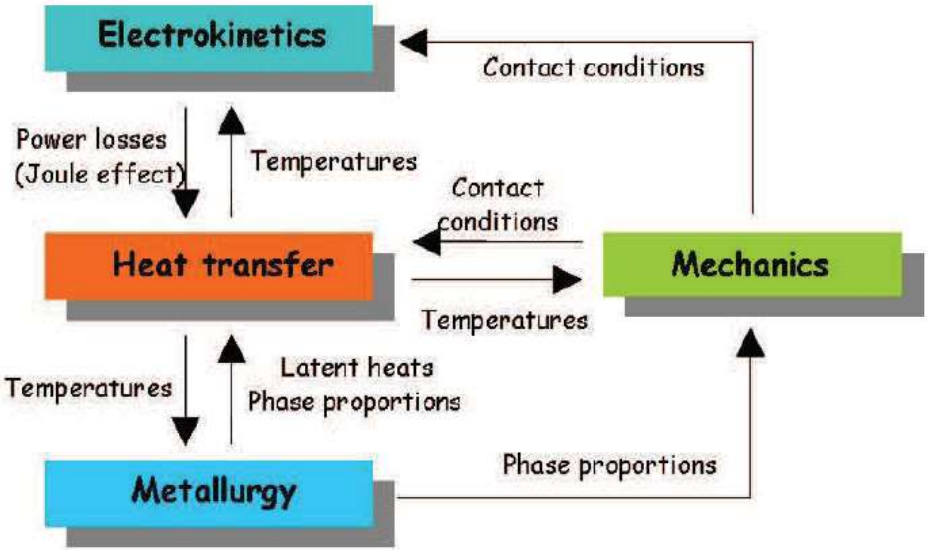

Figure 8: Coupling of RSW FE simulations

Electrical Governing Equations

As the main source of heat, due to the Joule heating, the electrical governing equations are presented first. To model the RSW process the steady-state electrokinetic problem can be used as an initial approach. The steady flow of current between the electrodes can be stated by Ohm's law in vector form, equation (11).

$$J = \kappa \nabla V \quad (11)$$

The current of a specific cross section of area is calculated as in equation (12).

$$I = \int J ds \quad (12)$$

In tandem with the principle of conservation of current flux, see equation (13), the above equations form the base of the electrical model.

$$\nabla J = 0 \quad (13)$$

Mechanical Modeling Equations

Given the computations of the electro-thermal modeling equations, the results can be used for the mechanical model. To establish the mechanical model the compatibility condition of the FE formulation is stated as in equations (14) and (15), respectively, representing normal and shear strains.

$$\varepsilon_r = \frac{\partial u_r}{\partial r}, \varepsilon_\theta = \frac{\partial u_\theta}{\partial \theta}, \varepsilon_z = \frac{\partial u_z}{\partial z} \quad (14)$$

$$\gamma_{rz} = \frac{\partial u_r}{\partial z} + \frac{\partial u_z}{\partial r} \quad (15)$$

The governing equation of the mechanical model can be expressed as in equation (16), representing a conventional elasto-plastic model.

$$\Delta\sigma = D\ \Delta\varepsilon + [C]\Delta T \quad (16)$$

The matrices [D] and [C] describe the elastic and thermo elasto-plastic states, respectively.

Boundary Conditions

In parallel with the governing equations, the model is based on a set of boundary conditions for the thermal, electrical and mechanical models. Each is treated separately below.

Electrical Boundary Conditions

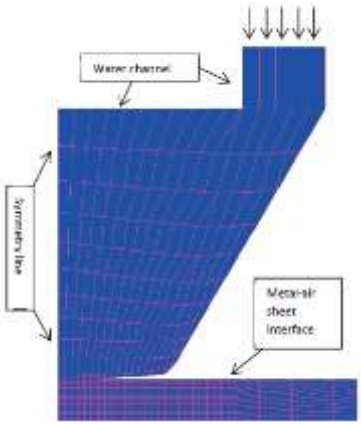

Figure 9: Boundary conditions associated with RSW FE simulations

The electrical boundary condition is a formulation of the applied welding current and the physical boundaries of the sheet, as shown in the following equations.

At the water channel J=0 (17)
At the symmetry line J=0 (18)
Top of upper electrode $V=V_e$ (19)
Bottom of lower electrode V=0 (20)
At the metal sheet surface facing air J=0 (21)

Thermal boundary conditions

The thermal boundary conditions are defined according to the following Equations

Heat loss at electrode-water interface,

$$-k\frac{\partial T}{\partial n} = K(T_w - T) \quad (22)$$

n is the normal direction of the boundary. The function *K(T)* is a combined function of the convection heat transfer coefficient and the radiation heat transfer coefficient.

Heat loss at metal sheet surface to air.

$$-k\frac{\partial T}{\partial n} = K(T_\infty - T) \quad (23)$$

T is the temperature of the surrounding medium, i.e. the air temperature. In the Sysweld model, *K(T)* includes both convective and radiation heat transfer closer to the electrodes but only convective heat transfer further away from the electrodes.

At symmetry lines.

$$-k\frac{\partial T}{\partial n} = O \quad (24)$$

Mechanical boundary Conditions

The mechanical boundary conditions are defined according to the following equations.

The pressure on the top of the upper electrode. $\sigma = -q$ (25)
The displacements at the bottom of the lower electrode. $U_z=0$ (26)
The displacements at the symmetry line. $U_r=0$ (27)

The stresses at the metal surfaces. σ = (28)

Boundary conditions after welding

As the hold time is finished and the electrodes are removed from the sheets a new set of boundary conditions are applied to the model. Firstly, the radiation component of the sheet surface heat transfer is neglected over the entire sheet, not only far from the electrodes as during welding [35-36]. Secondly, the electrical contact condition is removed. Thirdly, both electrodes are set to a vertical displacement of 3.0 mm away from the sheets.

III. Result and Discussions

The CT and MRI datasets we have taken here,

Temperature Distribution

For analysis of temperature distribution, parameters like contact area, preheating temperature, and distance from workpiece are changed.

The land width is modified by altering the plug size. The various graphs are displayed for temperature and workpiece distance. It can be seen that temperature is linearly decreasing, on decreasing land width.

As shown in figures 10, 11, 12 and 13, various Temperatures for pre-heating such as 350°C, 450°C, 550°C, and 650°C are indicated.

In figure 14 and 15, Temperature distribution vs displacement from contact surface with 16.0 mm and 4.0 mm land width is shown. It has been observed that temperature distribution is gradually decreasing with respect to the workpiece through its center point.

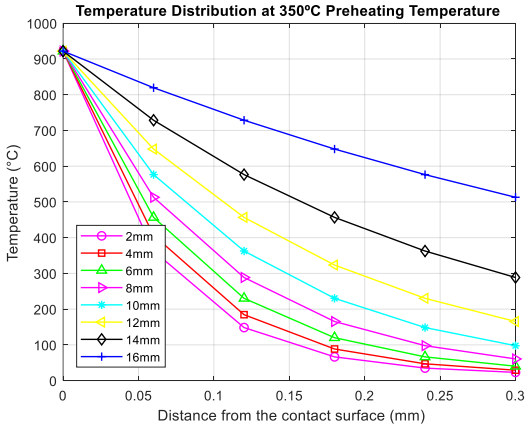

Figure 10: Temperature distribution at 350˚C preheating temperature

In figure 5.1, the maximum temperature distribution starts at 917˚C for different distance from workpiece at 350˚C preheating temperature.

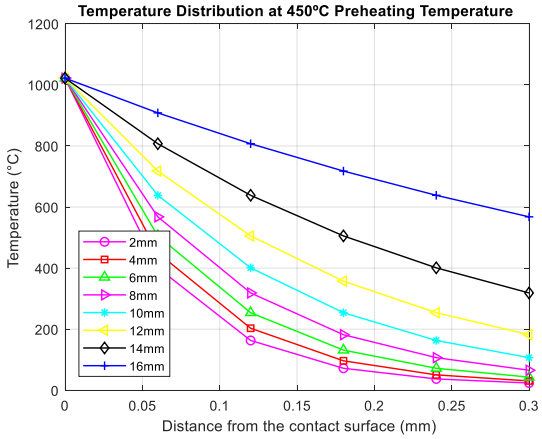

Figure 11: Temperature distribution at 450˚C preheating temperature

In figure 10, the maximum temperature distribution starts at 109˚C for different distance from workpiece at 450˚C preheating temperature.

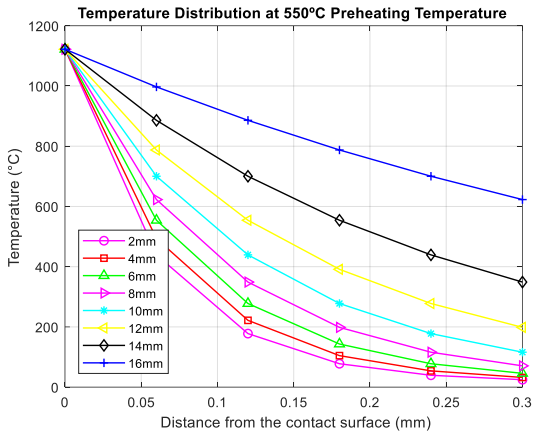

Figure 12: Temperature distribution at 550˚C preheating temperature

In figure 11, the maximum temperature distribution starts at 1132˚C for different distance from workpiece at 550˚C preheating temperature.

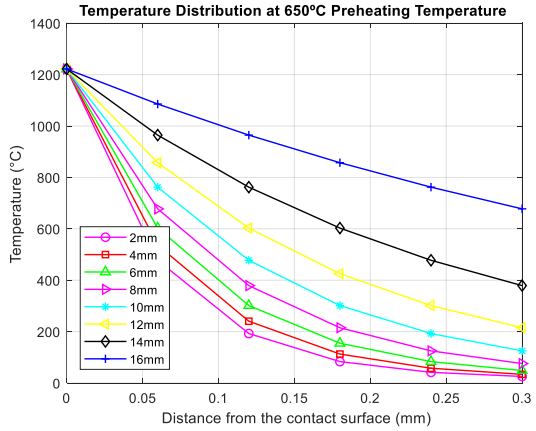

Figure 13: Temperature distribution at 650˚C preheating temperature

In figure 13, the maximum temperature distribution starts at 1222˚C for different distance from workpiece at 650˚C preheating temperature.

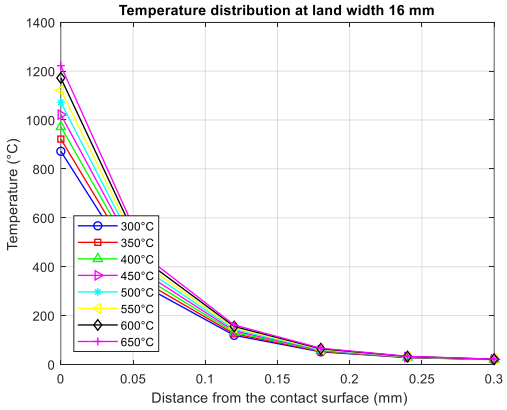

Figure 14: Temperature distribution at land width 16.0 mm

In figure 14, Temperature distribution is gradually decreasing with respect to the workpiece through its center point from contact surface at land width 16.0 mm.

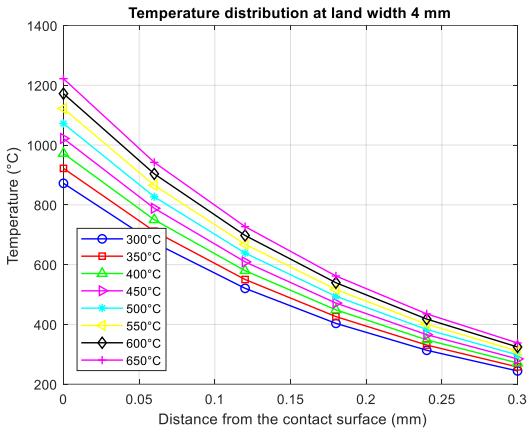

Figure 15: Temperature distribution at land width 4.0 mm

In figure 15, Temperature distribution is gradually decreasing with respect to the workpiece through its center point from contact surface at land width 4.0 mm. The decrement slope is lower than 16.0 mm.

Hardness Distribution analysis

As shown in figure 16, the Vicker's hardness profile of the welding process is presented. The hardness of the Thermo Mechanically Affected Zone (TMAZ), Heat-Affected Zone (HAZ), and Hard Zone (HZ) parent material region was computed. The hardness of the central zone was gradually less than the peripheral zone, and the hardness of the parent material was the lowest. The maximum value of hardness is at the central zone, shown in the TMAZ.

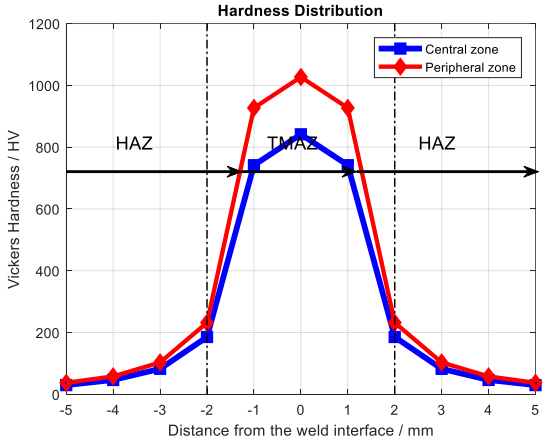

Figure 16: Hardness Distribution

As can be observed in figure 16, hardness decreases much slower in the HAZ and extends to 7 mm from the weld interface. The hardness value of this region ranged between 180 and 190 HV, which remained higher than that of the parent material.

The hardness value of the central zone was slightly lower than the one of the peripheral zone, and the hardness of the parent material was the lowest.

Ultimate Tensile Strength (UTS) of Resistance Spot Welding

As shown in figure 17, 18 and 19 graphs, used to understand the impact of RSW parameters on tensile strength like tool rotational speed, axial force, and welding speed.

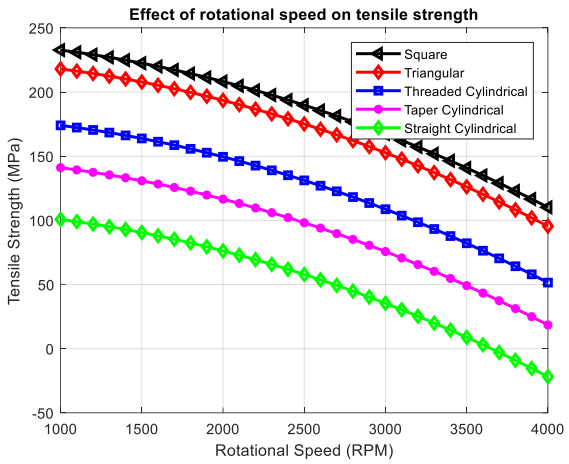

Figure 17: Effect of rotational speed on tensile strength

Figure 17 reveals the effect of tool rotational speed on tensile strength. At lower rotational speed (1500 RPM), the tensile strength of RSW joints is decreases. This trend is common in all the joints irrespective of tool pin profile.

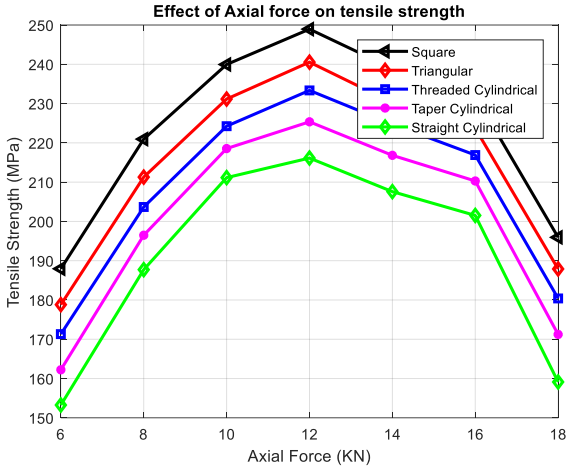

Figure 18: Effect of Axial force on tensile strength

Figure 18 reveals the effect of axial force on tensile strength of Resistance Spot welded. At lower axial force (6 KN) tensile strength of the RSW joints is lower. When the axial force is increased from 8 KN, correspondingly the tensile strength also increased and reaches a maximum at 12 KN. If the axial force is further increased above 12 KN, the tensile strength of the joint decreased. This trend is common in all the joints irrespective of tool pin profile.

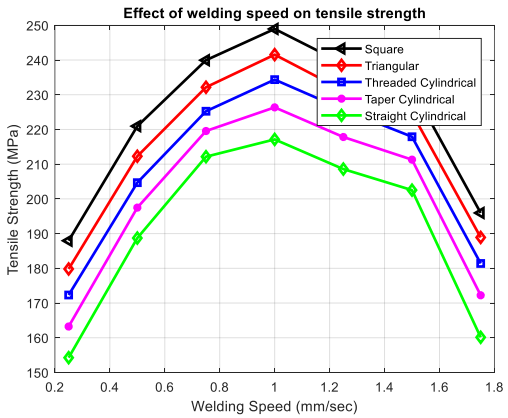

Figure 19: Effect of Welding Speed on tensile strength

Figure 19 reveals the effect of welding speed on tensile strength of Resistance Spot welding. At lower welding speed (0.25 mm/s), tensile strength of the RSW joints is lower. When the welding speed is increased from 0.25 mm/s, correspondingly the tensile strength also increased and reaches a maximum at 1.00 mm/s. If the welding speed is increased above 1.00 mm/s, the tensile strength of the joint decreased. This trend is common in all the joints irrespective of tool pin profile.

IV. Conclusion

The current thesis focuses on resistance spot welding process planning. Numerous studies have been conducted to address issues with spot weld size variability and the RSW process's numerical approaches' prediction power. The research' findings can be used to derive a number of conclusions. First, statistical analysis was performed on RSW weld size fluctuations. The studies demonstrated that weld sizes differ noticeably even under seemingly comparable circumstances. It was also observed that the extent of variances varied between manufacturing conditions and controlled laboratory conditions. Laboratory and production welds had standard deviations of about 0.3 and 0.9 millimetres, respectively. The distribution of weld sizes was further demonstrated through investigations on weld size changes. It was discovered that the distribution of weld diameters could be described by both normal and Weibull distributions in both laboratory and production settings. Additional research examined the RSW process' numerical approaches using FE simulations and regression models. By comparing the numerical approaches to actual welds, they were evaluated. Physical verification results for both models were encouraging. The regression models' standard deviations ranged from 0.5 mm to 0.7 mm, whereas the simulations' standard deviations were in the range of 0.7 mm.

References

[1] S. Oberthür and H. Ott, The Kyoto protocol, Berlin [u.a.]: Springer, 1999.

[2] P. Nieuwenhuis, A. Beresford and A. K.-Y. Choi, "Shipping or local production? CO2 impact of a strategic decision: An automotive industry case study," International Journal of Production Economics, vol. 140, no. 1, pp. 138-148, 2012.

[3] R. H. Borcherts, H. L. Stadler, W. M. Brehob and J. E. Auiler, "Improvements in Automotive Fuel Economy," Energy, vol. 3, pp. 439-449, 1978.

[4] A. Topolansky, "Alternative fuels: Challenges and opportunities for the global automotive industry," The Columbia Journal of World Business, vol. 28, no. 4, pp. 38-47, 1993.

[5] K. Edwards, "Strategic substitution of new materials for old: Applications in automotive product development," Materials & Design, vol. 25, no. 6, pp. 529-533, 2004.

[6] H. Zhang and J. Senkara, Resistance welding: fundamentals and applications, Boca Raton, Fla: CRC Press, 2006.

[7] M. Thornton, L. Han and M. Shergold, "Progress in NDT of resistance spot welding of aluminium using ultrasonic C-scan," NDT & E International, vol. 48, pp. 30-38, 2012.

[8] K. Benyounis and A. OIabi, "Optimization of different welding processes using statistical and numerical approches - A reference guide," Advances in Engineering Software, vol. 39, pp. 483-496, 2008.

[9] L. Lindgren, Computational welding mechanics: thermomechanical and microstructural simulations, Woodhead, 2007.

[10] T. Dupuy, "Estimation of SORPAS results scatter due to numerical parameters," in 6th International Seminar on Advances in Resistance Welding, Hamburg, 2010.

[11] M. Galler and W. Ernst, "The influence of electrode wear on current density IIW SC 27 09," IIW, 2009.

[12] P. Houldcroft, Feng, Fim and Fweldi, "Welding process developments and future trends," Materials & Design, vol. 7, no. 4, pp. 162-169, 1986.

[13] CMW, Resistance Welding Industries {@ONLINE}, 2012.

[14] G. Solas, J. Sharp and H. Goldsmid, Eds., Thermoelectrics. Basic Principles and New Materials Developments, Springer Heidelberg / New York, 2001.

[15] ISO 5821:2009 Resistance welding -- Spot welding electrode caps.

[16] ISO 5182:2008 Resistance welding -- Materials for electrodes and ancillary equipment.

[17] A. Rutqvist, An investigation of electrode degradation mechanisms to improve the electrode usage when spot welding, Goteborg: Chalmers tekniska högskola, 2005.

[18] I. Khan, M. Kuntz, L. Zhou, Y. Chan and N. K. Scotchmer, "Monitoring the Effect of RSW Pulsing on AHSS using FEA (SORPAS) Software," vol. 2139, pp. 37-44, 2007.

[19] W. Li, D. Cerjanec and G. A. Grzadzinski, "A comparative study of single-phase AC and multiphase DC resistance spot welding," Journal of Manufacturing Science and Engineering-Transactions of the Asme, vol. 127, no. 3, pp. 583-589, 2005.

[20] C. Ma, D. Chen, S. Bhole, G. Boudreau, A. Lee and E. Biro, "Microstructure and fracture characteristics," Materials Science and Engineering A, vol. 485, p. 334–346, 2008.

[21] O. Martin, P. D. Tiedra, M. Lopez and M. San-Juan, "Quality prediction of resistance spot welding joints of 304 austenitic stainless steel," Materials and Design, vol. 30, pp. 68-77, 2009.

[22] Y. Luo, J. Liu, H. Xu, C. Xiong and L. Liu, "Regression modeling and process analysis of resistance spot welding on galvanized steel sheet," Materials \& Design, vol. 30, no. 7, pp. 2547-2555, 2009.

[23] M. Zhou, H. Zhang and S. Hu, "Relationships between Quality and Attributes of Spot Welds," Welding Journal, vol. April, pp. 72s - 77s, 2003.

[24] H. Sahai and M. Ageel, The Analysis of Variance: Fixed, Random, and Mixed Models, Birkhäuser, 2000.

[25] G. Archer, "Calculations for temperature response in spot welds," Welding Journal, vol. 8, pp. 327s - 330s, 39.

[26] J. Greenwood, "Temperatures in spot welding," BWRA Report, pp. 316-322, 1960.

[27] Y. T. and T. Okudo, "A Study of Spot Welding of Heavy Gauge Mild Steel," Weldíng in the World, vol. 9, pp. 234-255, 1971.

[28] W. Rice and E. Funk, "An analytical investigation of the temperature distributions during resistance welding," Welding Journal, vol. 46, pp. 175s -186s, 1967.

[29] Z. Han, J. Orozco, J. E. Indacochea and C. H. Chen, "Resistance Spot Welding: A Heat Transfer Study," Welding Journal, vol. 68, pp. 363s - 371s, 1989.

[30] H. Cho and Y. Cho, "A study of the thermal behaviour in resistance spot welds," Welding Journal, vol. 68, no. 6, pp. 236s-244s, 1989.

[31] Reid, R., Prausnitz, J., & Poling, B. (1987). The properties of gases and liquids (4th ed.). New York: McGraw-Hill.

[32] Sun, Chunjing, Geng, Haoran, Ji, Leilei, Wang, Yan, & Wang, Guizhen. (2007). Rheological properties of Pb, Sb, Bi, and Sn melts. Journal of Applied Physics, 102(3).

[33] Way, Shaw, Wadhwa, & Busch. (2007). Shear rate dependence of viscosity and configurational entropy of the Zr 41.2Ti 13.8Cu 12.5Ni 10.0Be 22.5 metallic glass forming liquid. Journal of Alloys and Compounds, 434, 88-91

[34] Jeyakumar, M., Hamed, M., & Shankar, S. (2011). Rheology of liquid metals and alloys. Journal of Non-Newtonian Fluid Mechanics, 166(14–15), 831–838.

[35] FBejan, A., Kraus, A. D., Heat Transfer Handbook, John Wiley & Sons, Inc., 2003.